Supporting Information

Defect-Rich Amorphous Iron-Based Oxide/Graphene Hybrids Modified Separator towards Efficient Capture and Catalysis of Polysulfides

Yu Zhao[#a,b], Jiefei Liu[#a], Yu Zhou[a], Xiaofeng Huang[a], Qiqi Liu[a], Fuming Chen[a], Haiqing Qin[c], Hongtao Lou[d], Denis Y. W. Yu[b*], Xianhua Hou[a,d*]

a Guangdong Provincial Key Laboratory of Quantum Engineering and Quantum Materials, Guangdong Engineering Technology Research Centre of Efficient Green Energy and Environment Protection Materials, School of Physics and Telecommunication Engineering, South China Normal University, Guangzhou, 510006, China

b School of Energy and Environment, City University of Hong Kong, Hong Kong, China

c Guangxi Key Laboratory of Superhard Material, National Engineering Research Center for Special Mineral Material, China Nonferrous Metal (Guilin) Geology and Mining Co., Ltd., Guilin 541004, PR China

d Guangdong Lingguang New Material Co., Ltd, Zhaoqing, 526108, China

Tel: +(852)-3442-6885, E-mail addresses: denisyu@cityu.edu.hk (Denis Y.W. Yu)

Tel: +862039318011, E-mail addresses: houxianhua@m.scnu.edu.cn (X.H. Hou)

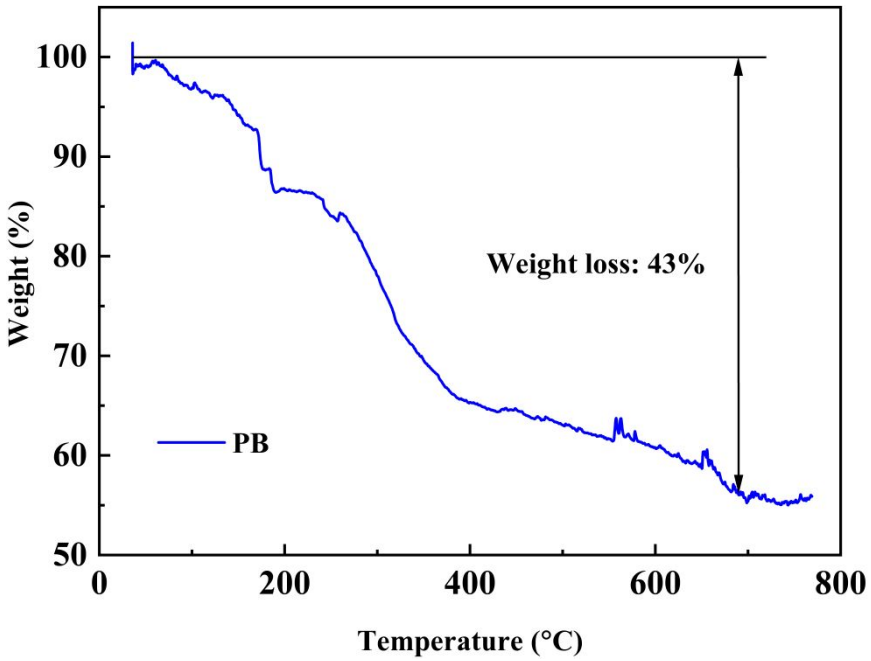

Figure S1. The TGA curve of pure PB.

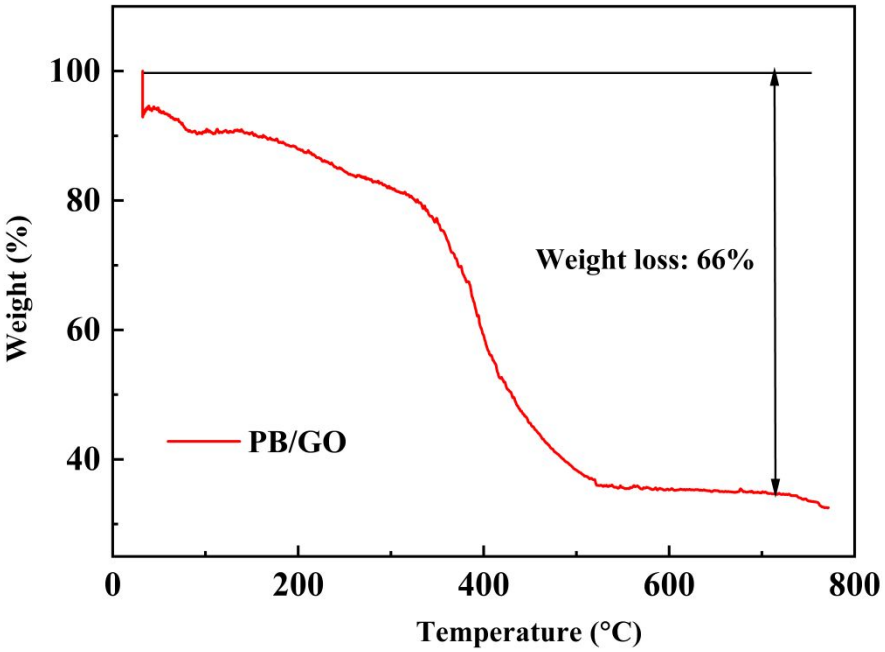

Figure S2. The TGA curve of PB/GO hybrid.

Table S1 A list of different peak position of Fe 2p in PB/GO and a-Fe_3O_{4-x}/GO.

Peak	**peak position in PB/GO (eV)**	**peak position in a-Fe_3O_{4-x}/GO (eV)**
Fe^{III} 2p 1/2	726.61	722.67
Fe^{II} 2p 1/2	724.32	720.92
Fe^{III} 2p 3/2	712.55	709.21
Fe^{II} 2p 3/2	710.72	708.00

Table S2 A content list of Fe in different valence state.

Fe state	**PB/GO (%)**	**a-Fe_3O_{4-x}/GO (%)**
Fe^{III} 2p 1/2	8.50	12.29
Fe^{II} 2p 1/2	9.37	11.64
Fe^{III} 2p 3/2	11.72	22.61
Fe^{II} 2p 3/2	18.32	16.41

All the percentage content of Fe are calculated based on area ratio.

Table S3. Comparison of the discharge specific capacities of a-Fe_3O_{4-x}/GO@PP separator at various current densities with those of other reported separator materials.

Materials	Reversible capacity (mAh g^{-1})				Reference
	0.1 C	0.2 C	0.5 C	1 C	
C@PI@LLZO separator	1169.3	-	815.8	679.8	[1]
PAN/GO separator	1268	445	382	303	[2]
GF separator	973	616	505	394	[3]
MoS_2 separator	1471	1039	770	550	[4]
Tree-like F-doped PMIA membrane	1237	962	820	750	[5]
Vermiculite separator	930	810	730	700	[6]
Ti_3C_2 nanosheet/GF separator	1462	886	716	530	[7]
a-Fe_3O_{4-x}/GO separator	**1313**	**980**	**834**	**695**	**This work**

Reference:

[1] Zhenfang, Z.; Tingkai, Z.; Xionggang, L.; Huaqing, C.; Xu, Z.; Zhongfu, Z., Functionalized polyimide separators enable high performance lithium sulfur batteries at elevated temperature, *J. Power Sources*, **2018**, *396*, 542-550.

[2] Lei, T.; Chen, W.; Hu, Y.; Lv, W.; Lv, X.; Yan, Y.; Huang, J.; Jiao, Y.; Chu, J.; Yan, C.; Wu, C.; Li, Q.; He, W.; Xiong, J., A Nonflammable and Thermotolerant Separator Suppresses Polysulfide Dissolution for Safe and Long-Cycle Lithium-Sulfur Batteries, *Adv. Energy Mater.*, **2018**, *8*, 1802441.

[3] Jiadeng, Z.; Yanilmaz, M.; Kun, F.; Chen, C.; Yao, L.; Yeqian, G.; David, K.; Xiangwu, Z.; Understanding glass fiber membrane used as a novel separator for lithium–sulfur batteries, *J. Membr. Sci.*, **2016**, *504*, 89-96.

[4] Ghazi, Z. A.; He, X.; Khattak, A. M.; Khan, N. A.; Liang, B.; Iqbal, A.; Wang, J.; Sin, H.; Li, L.; Tang, Z. MoS_2/Celgard Separator as Efficient Polysulfide Barrier for Long-Life Lithium-Sulfur Batteries. *Adv. Mater.*, **2017**, *29 (21)*, 1606817.

[5] Nanping, D.; Yan, W.; Mgji, Y.; Jingge, J.; Zongjie, L.; Lanlan, F.; Huijuan, Z.; Weimin, K.; Bowen, C., A F-doped tree-like nanofiber structural poly-m-phenyleneisophthalamide separator for high-performance lithium-sulfur batteries, *J. Power Sources*, **2017**, *362*, 243-249.

[6] Rui, X.; Yingzhi, S.; Yunfei,W.; Jiaqi, H.; Qiang, Z., Two-dimensional vermiculite separator for lithium sulfur batteries, *Chinese Chem. Lett.*, **2017**, *28 (12)*, 2235-2238

[7] Lin, C.; Zhang, W. K.; Wang, L.; Wang, Z. G.; Zhao, W.; Duan, W. H.; Zhao, Z. G.; Liu, B.; Jin, J. A few-layered Ti_3C_2 nanosheet/glass fiber composite separator as a lithium polysulphide reservoir for high-performance lithium-sulfur batteries. *J. Mater. Chem. A*, **2016**, *4 (16)*, 5993-5998.

Table S4 A list of calculated diffusion coefficient for Li^+ from at peak A, B and C.

Diffusion coefficient	**PP separator ($cm^2\ s^{-1}$)**	**a-Fe_3O_{4-x}/GO@PP separator ($cm^2\ s^{-1}$)**
D_{Li^+} from peak A	5.71×10^{-14}	2.00×10^{-12}
D_{Li^+} from peak B	2.00×10^{-14}	2.72×10^{-13}
D_{Li^+} from peak C	2.26×10^{-14}	5.20×10^{-13}

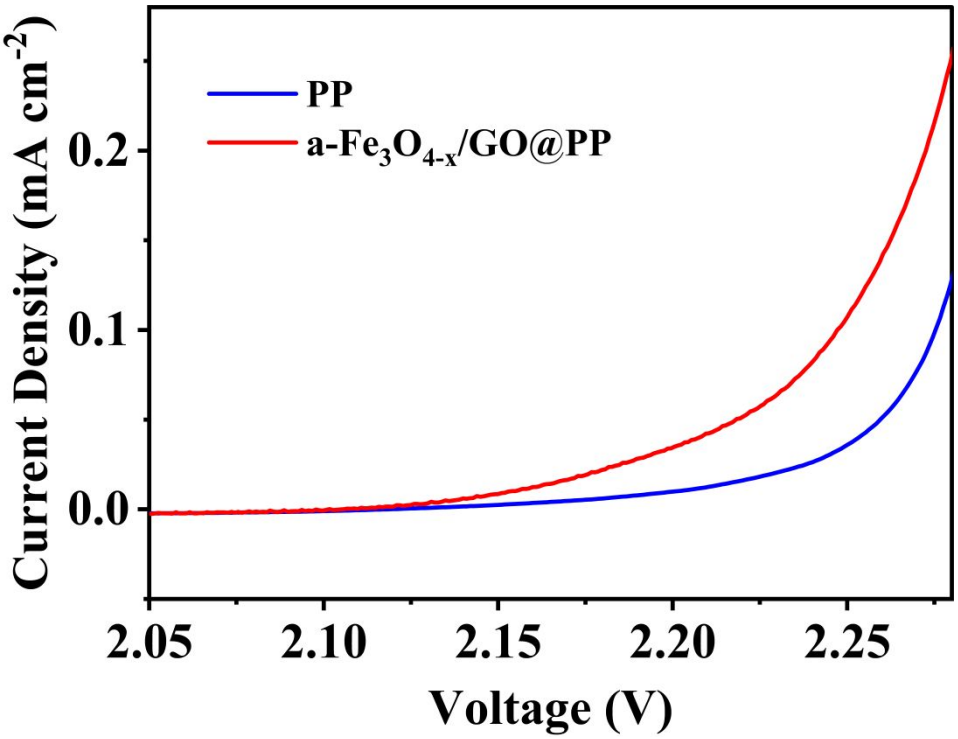

Figure S3. LSV curves for peak A of PP and a-Fe_3O_{4-x}/GO@PP separators.

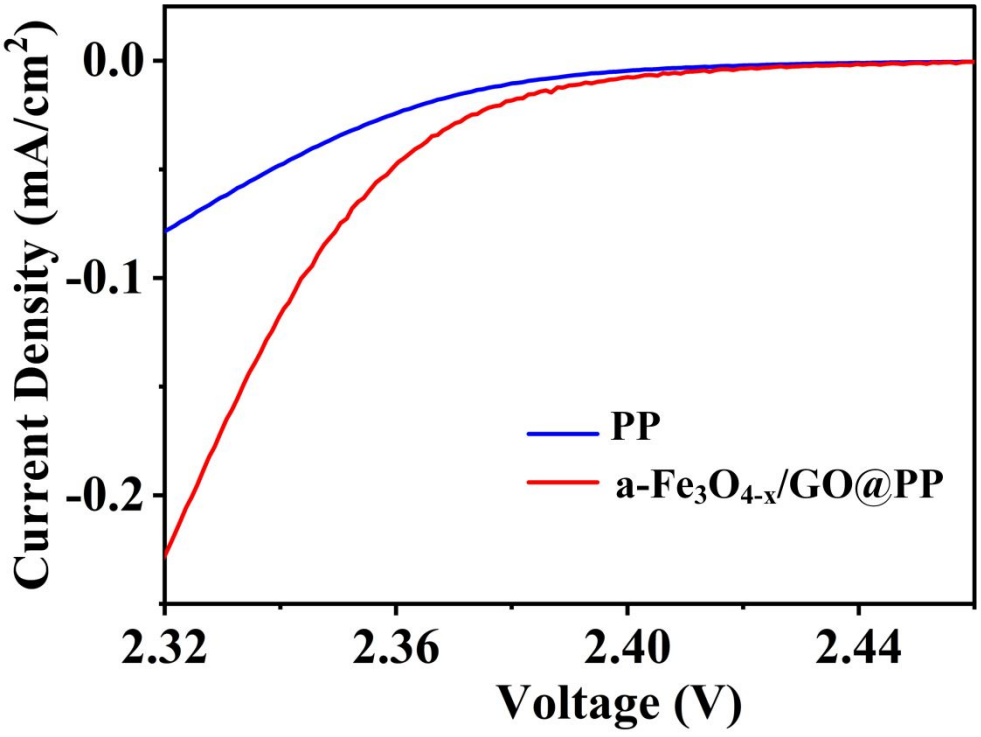

Figure S4. LSV curves for peak B of PP and a-Fe_3O_{4-x}/GO@PP separators.

Tafel slope calculation method:

The Tafel slopes are calculated using the equation: $\eta=a \log J+b$ where η (V) is the experimental overpotential, J (mA cm^{-2}) means the experimental current density, and a is for the Tafel slope, b is a constant that depends primarily on temperature.

Then, the Tafel slopes are obtained via the following four steps:

1. take one LSV curve within a particular voltage range.
2. convert the current to current-density (J) and then take the absolute value of the current density data.
3. take log value of the absolute current density value.
4. plot the log value as X axis and voltage as Y axis to get the Tafel plot. The Tafel slope is obtained by fitting the top portion of the Tafel plot with a straight line.